International Journal of Heat and Technology
Vol. 42, No. 4, August, 2024, pp. 1317-1326
Journal homepage: http://iieta.org/journals/ijht

Application of Thermodynamic Models in Bridge Temperature Field Simulation and Thermal Stress Analysis

Junping Bian[1], Yueliang Wang[1], Yanyan Li[2*]

[1] China First Highway Engineering CO., LTD., Beijing 100024, China
[2] College of Civil Engineering, Xuchang University, Xuchang 461000, China

Corresponding Author Email: 22005001@xcu.edu.cn

https://doi.org/10.18280/ijht.420422

Received: 15 February 2024
Revised: 7 June 2024
Accepted: 28 June 2024
Available online: 31 August 2024

Keywords:
bridge temperature field, thermal stress, thermodynamic model, numerical simulation, structural safety

ABSTRACT

As modern bridge structures evolve towards lighter weight and longer spans, the impact of temperature effects on their safety and durability has become increasingly significant. Temperature-induced thermal stress can greatly affect the stability of bridge structures, particularly under extreme climatic conditions, where uneven temperature distribution can lead to substantial temperature gradients, stress concentrations, and fatigue damage. Therefore, conducting numerical simulations of bridge temperature fields and thermal stress analysis is of critical importance. Although existing thermodynamic models are widely applied in bridge temperature field and thermal stress analyses, they still exhibit limitations in accounting for material thermal property variations, multi-scale temperature effects, and boundary condition handling, which restricts the accuracy and applicability of the analysis results. This paper proposes an improved numerical simulation method for bridge temperature fields based on thermodynamic principles and incorporates thermal stress analysis under complex climatic conditions. The aim is to enhance simulation accuracy and provide more scientific evidence for bridge design and maintenance.

1. INTRODUCTION

In modern bridge engineering, temperature effects have a significant impact on the safety and durability of bridge structures [1-4]. As bridge design gradually trends towards lightweight and large-span structures, the issue of thermal stress induced by temperature changes has increasingly become an important factor affecting the health of bridge structures. Especially under extreme climatic conditions, the uneven distribution of the temperature field in bridge structures can cause large temperature gradients, leading to thermal stress, which results in stress concentration or fatigue damage to the bridge structure [5,6]. Therefore, accurate simulation of the bridge temperature field and thermal stress analysis has become an important research topic to ensure the safety of bridge structures and extend their service life.

Relevant studies have shown that using thermodynamic models to analyze bridge temperature fields and thermal stress can not only help engineers better understand the temperature response of bridges under different climatic conditions but also provide a scientific basis for bridge design and maintenance [7-10]. This research is of great significance in the design, construction, and operation of bridges, as it can effectively reduce the risk of structural damage caused by temperature changes and improve the overall reliability and economic efficiency of bridges.

Although many studies have applied thermodynamic models to analyze bridge temperature fields and thermal stress, existing methods still have certain deficiencies in terms of accuracy and applicability [11-14]. For example, traditional temperature field simulation methods often neglect the thermal property variations of bridge materials or fail to fully consider the multi-scale temperature effects under complex climatic conditions [15, 16]. In addition, in terms of boundary condition treatment in thermal stress analysis and the determination of model parameters, existing research methods also lack systematicness and precision, leading to a need for improvement in the reliability of the analysis results [17-21].

This paper aims to address these deficiencies by proposing a numerical simulation method for bridge temperature fields based on thermodynamics and combining it with bridge thermal stress analysis to explore the impact of temperature changes on bridge structures in depth. The research mainly includes two aspects: first, the numerical simulation study of the bridge temperature field based on thermodynamics, which improves the accuracy of temperature field simulation by introducing a multi-scale simulation method and considering material thermal property variations; second, the thermodynamic-based bridge thermal stress analysis, focusing on the distribution laws of thermal stress under complex climatic conditions. Through this research, it is expected to provide more scientific reference bases for bridge design and maintenance and to promote new progress in temperature effect research in the field of bridge engineering.

2. THERMODYNAMIC-BASED NUMERICAL SIMULATION OF BRIDGE TEMPERATURE FIELDS

2.1 Internal parameters

In bridge structures, the thermal conduction characteristics of different materials, such as concrete, steel, and gravel, vary under conditions of sudden cooling and radiative heating. Therefore, accurately selecting the internal parameters of these materials' thermal conduction is crucial. Specifically, as the main load-bearing material of bridges, the thermal conductivity, specific heat capacity, and density of concrete under sudden cooling conditions need to account for the freezing effect of internal moisture. Frozen moisture can significantly increase the thermal conductivity of concrete, and due to differences in thermal expansion coefficients, it may lead to internal stress concentrations, thus affecting structural safety. Therefore, under sudden cooling conditions, the thermal conductivity of concrete can depend on its moisture content and the relationship between temperature changes, while the specific heat capacity needs to be calculated by considering the differences in heat capacity between frozen and unfrozen states.

For steel, under conditions of sudden cooling and radiative heating, its thermal conduction characteristics are mainly influenced by thermal conductivity and specific heat capacity. The thermal conductivity of steel is typically high, and during drastic temperature changes, the internal temperature gradient in steel can easily induce thermal stress. Under sudden cooling, the value of steel's thermal conductivity should consider its low-temperature performance and take into account the material hardening effect caused by temperature changes. During radiative heating, the thermal conductivity and specific heat capacity of steel should be adjusted according to the rate of temperature rise and radiation intensity to ensure rapid heat dissipation and avoid local overheating.

As a foundational material in bridges, the thermal conduction characteristics of gravel under conditions of sudden cooling and radiative heating are significantly influenced by porosity and particle distribution. Under sudden cooling, the thermal conductivity of gravel can be determined based on its density and porosity, with particular consideration given to the enhancement of thermal conductivity due to the freezing of moisture in the pores. Under radiative heating conditions, the thermal conductivity of gravel should consider changes in surface temperature and the contact thermal resistance between particles, while the specific heat capacity value should be adjusted based on changes in heat capacity at different temperatures. Additionally, the changes in the thermal expansion coefficient of gravel under these two extreme temperature conditions are also important factors affecting thermal conduction and should be considered when determining parameter values.

2.2 External parameters

(1) Convective Heat Transfer

Convective heat transfer is a crucial process in bridges under sudden cooling and radiative heating, directly affecting the changes in bridge surface temperature and the distribution of the internal temperature field. Figure 1 illustrates the heat transfer process in a bridge. In bridge structures, the convective heat transfer coefficient g_z and ambient temperature S_x are key parameters determining the intensity of convective heat transfer. Since bridges are usually exposed to the natural environment, there is a temperature difference between the bridge surface temperature S and the surrounding air temperature S_x, leading to convective heat transfer between the bridge surface and the flowing air. This process needs to be accurately described in the simulation of the bridge temperature field to ensure the reliability of the calculation results.

The convective heat transfer coefficient g_z is a parameter that describes the transfer of heat from the bridge surface to the surrounding fluid or vice versa. Its magnitude depends on the flow state of the fluid, the roughness of the bridge surface, and the physical properties of the fluid. In bridge engineering, wind speed, wind direction, and the characteristics of the bridge surface have a significant impact on g_z. For the upper structure of a bridge, the wind speed is usually higher, which may lead to a higher convective heat transfer coefficient; while for the lower structure of a bridge, due to lower wind speed, the convective heat transfer coefficient is relatively smaller. When performing numerical simulations of the temperature field, it is necessary to reasonably select the value of g_z based on the specific location of the bridge, environmental conditions, and fluid dynamics characteristics to accurately reflect the actual intensity of convective heat transfer.

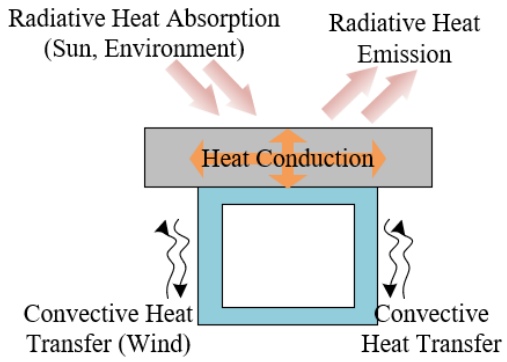

Figure 1. Bridge heat transfer diagram

Assuming that the basic value of the convective heat transfer coefficient in a windless state is represented by X, the wind speed influence coefficient of the convective heat transfer coefficient is represented by Y, and the ambient wind speed is represented by n, the convective heat transfer coefficient is calculated by the following formula:

$$g_z = X + Yn \tag{1}$$

Further considering the influence of wind speed, bridge structure surface temperature, and ambient temperature on the convective heat transfer coefficient, the formula can be adjusted to:

$$g_z = 2.6\sqrt[4]{|S - S_x|} + 4n \tag{2}$$

where, S_x is another important parameter in the numerical simulation of the bridge temperature field, reflecting the temperature conditions of the environment where the bridge is located. Bridges are usually exposed to the atmospheric environment, and the ambient temperature not only changes over time but may also be affected by seasonal, geographical, and meteorological conditions. For example, in cold seasons

or at night, the ambient temperature is relatively low, which may cause the bridge surface to cool rapidly; while in summer or during the day, the ambient temperature rises, which may cause the bridge surface temperature to increase. Therefore, when simulating the bridge temperature field, S_x needs to be dynamically adjusted according to actual meteorological data to accurately simulate the bridge's temperature response under different time periods and seasonal conditions.

(2) Radiative Heat Transfer

Radiative heat transfer is one of the important means of energy exchange between the bridge and the external environment. Radiative heat transfer includes two processes: radiative heat absorption and radiative heat emission. These processes play a key role in the formation and development of the bridge temperature field, especially under extreme climatic conditions. Figure 2 illustrates the radiative heat transfer process in a bridge.

Radiative heat absorption mainly involves the bridge's absorption of solar radiation. Solar radiation is one of the main sources of external heat absorbed by the bridge, especially during the day and in hot seasons, where the bridge surface temperature can significantly increase due to the effect of solar radiation. The ability of bridge materials to absorb solar radiation is determined by their absorptivity, which depends on the material's color, surface roughness, and optical properties. For example, dark-colored materials usually have higher absorptivity, leading to greater heat accumulation on the bridge surface, while light-colored or polished materials can reflect more solar radiation, reducing the amount of heat absorbed. In numerical simulation of the temperature field, it is necessary to accurately determine the absorptivity of bridge materials to correctly calculate the impact of solar radiation on bridge temperature. Accurate modeling of absorptivity helps simulate the temperature changes of the bridge under different times and weather conditions, providing important references for bridge design. Assuming the absorptivity of an object is represented by β, and the intensity of thermal radiation is represented by U, the calculation formula is:

$$w_t = \beta U \tag{3}$$

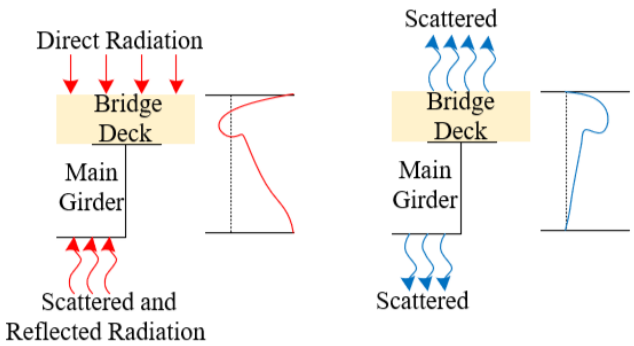

Figure 2. Bridge radiative heat transfer diagram

Radiative heat emission involves the bridge radiating heat to the external environment. According to the law of blackbody radiation, the amount of radiative heat emission from the bridge surface depends on the difference between its temperature and the ambient temperature, as well as the emissivity of the material. The emissivity of bridge materials reflects their ability to release heat in the form of radiation. Materials with high emissivity can accelerate the heat dissipation of the bridge, helping to reduce the bridge surface temperature at night or in cold weather, thereby reducing thermal stress and fatigue damage caused by overheating. However, radiative heat emission can also lead to excessive cooling of the bridge surface in some cases, especially in cold seasons or at night, which may increase the risk of low-temperature thermal stress. In temperature field simulation, the calculation of radiative heat emission needs to consider the emissivity of the bridge surface material and the impact of environmental conditions on thermal radiation. Assuming the emissivity of an object is represented by γ, and the Stefan-Boltzmann constant is represented by Z_t, the calculation formula is:

$$w_e = \gamma Z_s \left[(S + 273.15)^4 - (S_x + 273.15)^4 \right] \tag{4}$$

(3) Contact Heat Transfer

Contact heat transfer between the steel bridge and the concrete slab is an important factor affecting the temperature field distribution of composite bridges. Due to the presence of a contact surface between steel and concrete, this contact surface is often not in perfect contact, leading to the appearance of contact thermal resistance, which in turn affects the transfer of heat flow. The presence of contact thermal resistance means that the transfer of heat between the steel bridge and the concrete slab is hindered, a phenomenon that needs to be considered as a fourth-type boundary condition in temperature field analysis. Specifically, contact thermal resistance is determined by the interfacial characteristics between the steel bridge and the concrete slab, and its value depends on various factors such as the mechanical and thermal properties of the contact materials, surface roughness, contact pressure, interfacial temperature, the presence of interfacial media, and the chemical bonding conditions at the interface. Research has shown that the larger the contact thermal resistance, the more difficult it is for heat to transfer between the steel bridge and the concrete slab, resulting in an increase in the temperature difference across the interface. In bridge temperature field simulation, it is necessary to select an appropriate value for contact thermal resistance based on actual conditions to accurately reflect the heat transfer characteristics of the steel-concrete interface. Therefore, the influence of contact thermal resistance on heat flux density is a key point in temperature field simulation. Due to the presence of contact thermal resistance, the heat flux density at the steel bridge and concrete slab interface will be limited, leading to an increase in the temperature gradient at the interface. According to thermodynamic theory, the heat flux density at the interface can be calculated using a specific formula, which needs to consider the properties of the contact materials and the actual pressure on the contact surface. When experimental conditions are insufficient to directly measure contact thermal resistance, it can be estimated through theoretical calculations or based on data from existing literature. In specific simulations, if materials such as 1mm synthetic fibers are used at the interface, the characteristics of these materials also need to be included in the calculation of contact thermal resistance to ensure the accuracy of the simulation. Assuming the thermal conductivity of the contact material is represented by η, and the contact thermal resistance is represented by E_z, the heat flux density at the steel-concrete interface can be calculated by the following formula:

$$\overline{w} = \eta \frac{\partial S}{\partial v} = \frac{\Delta S}{E_z} \tag{5}$$

Contact thermal resistance can be calculated by the following formula:

$$E_z = \frac{\Delta v}{\eta} = \frac{0.001}{0.04} = 0.025\, m^2 \cdot °C/W \tag{6}$$

2.3 Model establishment

(1) Model Dimensions

Although the temperature along the longitudinal direction of a bridge can generally be considered uniformly distributed, and a two-dimensional model can significantly reduce computational resource consumption, a two-dimensional model cannot accurately reflect the non-uniformity of surface radiative intensity during radiative heating. Additionally, the presence of stud groups in the bridge also significantly affects the temperature field, and these factors are difficult to fully represent in a two-dimensional model. Therefore, this paper adopts a three-dimensional model for temperature field simulation to more precisely capture the temperature distribution characteristics of bridge structures under complex thermal conditions. The use of a three-dimensional model not only better reflects the impact of radiative heat transfer on the bridge surface but also accurately describes the local effects of internal structures, such as stud groups, on the temperature field.

(2) Elements and Meshes

For element and mesh division, this paper selects the DC3D8 element provided in ABAQUS software. The DC3D8 element is an 8-node heat transfer solid element suitable for linear diffusion problems. The main reason for choosing this element is that it can reduce computational load while ensuring the accuracy of the simulation. In the simulation of the bridge temperature field, the mesh is reasonably divided to ensure that the overall model is suitable for the DC3D8 element and maintains a high mesh quality. High-quality mesh division can effectively reduce computational errors and ensure the reliability of the results. At the same time, reasonable mesh division can also enable the model to exhibit higher accuracy in local details, such as the contact surface between the bridge and the environment or the handling of internal complex structures.

(3) Steel-Concrete Connection Handling

Composite bridge structures usually consist of a steel bridge and a concrete slab, and the handling of the connection between the two directly relates to the accuracy of the simulation results. To consider the impact of contact thermal resistance and the contribution of the stud group to the temperature field, this paper adopts the following approach. First, studs are established on the steel bridge, and the concrete slab is connected to the studs through Embedded region constraints. Then, in ABAQUS's Interaction module, the contact relationship between the steel bridge and the concrete slab interface is defined through Surface-to-surface contact. In the setting of contact properties, the thermal conductivity of the interface is defined to reflect the possible thermal resistance effects on the contact surface. This approach can accurately account for contact thermal resistance and effectively simulate the impact of the stud group on the temperature field, thereby providing more accurate simulation results. The following formula gives the calculation of the thermal conductivity of the interface in the contact properties:

$$\overline{\eta} = \frac{1}{E_z} = \frac{1}{0.035} = 28.57 W/\left(m^2 \cdot °C\right) \tag{7}$$

(4) Nonlinear Thermal Boundaries

Bridge structures in natural environments are affected by various complex thermal boundary conditions, such as convective heat transfer and radiative heat transfer, which have significant nonlinear characteristics. Therefore, they need to be precisely defined and set in the finite element model.

For convective heat transfer on the bridge surface, this paper uses the Interaction module in ABAQUS for definition. The convective heat transfer coefficient g_z is not a fixed value but a function of the bridge surface temperature and ambient temperature. Therefore, to accurately simulate this dynamic relationship, this paper uses the user subroutine FILM to define the convective heat transfer coefficient. Through this subroutine, the precise calculation of the bridge surface temperature as it changes with ambient temperature can be achieved, and the convective heat transfer coefficient can be dynamically adjusted to ensure that the simulation process accurately reflects the actual situation.

In the setting of radiative heat transfer, key parameters include emissivity γ and ambient temperature S_x, which are also defined in the Interaction module. Particularly, the ambient temperature S_x, which changes over time, is set using the Amplitude tool in ABAQUS to achieve an accurate description of temperature changes during different time periods. Additionally, in the model properties, the Stefan-Boltzmann constant and absolute zero must also be defined, as these physical constants play a fundamental supporting role in radiative heat transfer calculations. The definition of radiative heat absorption is completed through the Load module, where the distribution of surface heat flux is set using the Analytical Field tool. Measured radiative values for each point are input to form a thermal radiation cloud dataset, which more intuitively presents the distribution of radiative heat intensity across different regions of the bridge. To simulate the bridge's state changes under different thermal environments, the Amplitude tool is also used to set up the radiative heating stage and natural cooling stage, making the thermal boundary conditions more dynamic and adaptable to actual conditions.

In addition to the boundary definitions for convective and radiative heat transfer, the initial thermal state of the model is also crucial. In the Load module of ABAQUS, the initial temperature S_0 is set through the Predefined Field function to ensure that the simulation starts from a reasonable initial temperature state, which plays a fundamental role in the evolution of the entire temperature field.

(5) Analysis Step Settings

Transient thermal analysis aims to capture the dynamic process of temperature changes at various points in the bridge structure over time, and it is an important means of reflecting the temperature field distribution of the bridge under different thermal conditions. Therefore, reasonable setting of analysis steps is crucial to ensuring the accuracy and convergence of the simulation. In this study, the heat transfer process of the

composite bridge is a typical transient thermal process, with temperatures at various points changing over time. To this end, the steps for transient thermal analysis are defined through the Step module in ABAQUS during the establishment of the finite element model. The core of transient thermal analysis is the selection of the time step, which directly impacts the convergence of the computation and the accuracy of the results. Based on the specific conditions of the bridge under different thermal conditions, the analysis is divided into two scenarios: heating and cooling. In the cooling scenario, considering the relatively slow temperature changes, the time step is set to 1 hour, which allows for capturing the gradual changes in the temperature field while ensuring computational efficiency. In the heating scenario, due to the relatively rapid temperature changes, the time step is set to 0.2 hours to ensure detailed recording of the rapid temperature rise process. By reasonably setting the time steps under different conditions, the balance between computational accuracy and convergence can be effectively maintained, ensuring that the transient thermal analysis can accurately reflect the dynamic changes in the bridge temperature field. Additionally, the total duration of the analysis step is set according to actual conditions, ensuring that the entire heat transfer process is fully reflected in the simulation. The choice of time step not only considers the convergence of the solution but also meets the requirements for result accuracy. This method of setting the time step according to different thermal conditions allows the model to perform effective transient thermal analysis in complex thermal environments, thereby providing a scientific basis for predicting the temperature field of the bridge.

3. THERMODYNAMIC-BASED THERMAL STRESS ANALYSIS OF BRIDGES

3.1 Temperature strain of bridge surface concrete under high temperature

In the thermodynamic-based numerical simulation study of the bridge temperature field, the temperature strain of the bridge surface concrete under high temperature is a crucial factor affecting the overall structural safety and durability of the bridge. Temperature strain mainly includes free expansion strain γ_{sg} and transient thermal strain γ_{se}. Their values are usually large under high-temperature conditions, making them key influencing factors in the coupled constitutive relationship and the main part of the overall deformation of the bridge under high temperature.

In practical applications, the temperature strain of bridge concrete is influenced by various factors, among which the difference in the coefficient of linear expansion between the reinforcement and concrete plays a significant role. As the temperature rises, thermal stress gradually develops between the concrete and the internal reinforcement, especially when the temperature reaches below 150°C, where the temperature strain of the bridge surface concrete is significantly greater than the value predicted by the conventional concrete deformation formula. This difference is mainly due to the additional strain generated by the reinforcement being constrained by the concrete during the heating process, which in turn affects the overall temperature strain behavior. Specifically, the coefficient of linear expansion of the reinforcement is greater than that of the concrete, meaning that during the heating process, the reinforcement will expand faster, thereby being constrained by the surrounding concrete. This constraint force generates additional thermal stress, resulting in a larger temperature strain value of the concrete before 150°C. Figure 3 shows the schematic diagram of the thermodynamic-based thermal stress analysis model adopted in this paper.

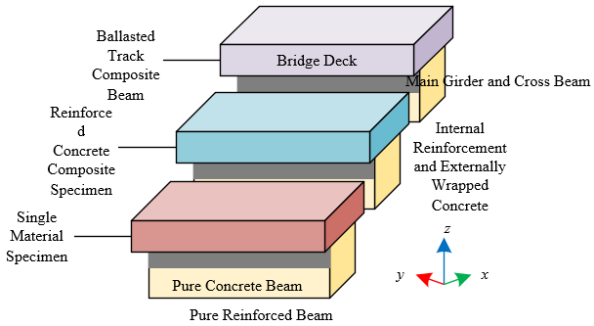

Figure 3. Thermodynamic-based thermal stress analysis model

When the temperature exceeds 150°C, the bond between the internal reinforcement and the concrete begins to weaken and gradually fails, so the concrete can no longer effectively restrict the deformation of the reinforcement. At this point, the temperature strain of the bridge surface concrete approaches free temperature strain, and the difference between the two gradually decreases, with the temperature strain curve tending to coincide with the predicted curve of the concrete. This indicates that under high-temperature conditions, the thermal coupling effect between the reinforcement and concrete has a decisive influence on the overall deformation of the bridge.

3.2 Temperature strain of internal reinforcement under high temperature

The deformation of reinforcement in a high-temperature environment is not only directly related to temperature but is also closely related to the stress coupling between the reinforcement and concrete, which makes the temperature strain of the reinforcement exhibit complex characteristics.

From a thermodynamic perspective, the deformation of reinforcement under high-temperature conditions can be decomposed into three parts: free expansion strain, transient high-temperature creep, and short-term high-temperature creep. Free expansion strain is the natural expansion of the reinforcement as the temperature rises without external constraint. However, in an actual bridge structure, the reinforcement does not exist independently but is tightly bonded with the surrounding concrete, and this bond under high temperature will trigger a complex stress-strain relationship.

Specifically, within the temperature range of 30°C to 90°C, as the temperature rises, the reinforcement inside the bridge undergoes compressive deformation due to the constraint of the concrete, which is contrary to the trend of free expansion strain. This compressive deformation is a result of the thermal coupling effect between the reinforcement and concrete, reflecting the constraint effect of the concrete on the reinforcement. However, when the temperature rises to between 90°C and 110°C, the compressive deformation of the reinforcement rapidly decreases and gradually recovers to and exceeds the level of free expansion strain, indicating an increase in the expansion rate of the reinforcement within this

temperature range. This may be due to the weakening of the bond between the reinforcement and concrete in this temperature range, allowing the deformation of the reinforcement to no longer be fully constrained by the concrete, thereby fully releasing the expansion deformation.

When the temperature further increases above 110℃, the expansion rate of the reinforcement inside the bridge approaches free expansion, indicating that in a high-temperature environment, the deformation of the reinforcement gradually approaches its natural thermal expansion behavior. However, experimental data show that under the combined effect of high thermal stress and temperature, the actual deformation of the reinforcement is much greater than the free expansion strain, indicating that significant transient high-temperature creep and short-term high-temperature creep also occur in the reinforcement under high-temperature conditions. These creeps are due to the gradual changes in the internal structure of the reinforcement and stress relaxation under high temperatures, which are the result of the coupling effect of stress and temperature under high-temperature conditions.

3.3 Axial thermal stress of reinforcement and concrete in bridges

Furthermore, this paper achieves a comprehensive understanding of the thermal stress distribution in reinforced concrete structures under thermodynamic conditions and its impact on bridge safety by analyzing the axial stress of reinforcement, the axial stress of concrete, and the axial thermal stress at concrete measuring points in the bridge.

The axial stress of reinforcement in a bridge mainly originates from the thermal expansion or contraction caused by temperature changes. Since the coefficient of linear expansion of reinforcement is generally greater than that of concrete, during the heating process, the reinforcement attempts to expand, while the surrounding concrete exerts a constraint effect on it, generating axial stress within the reinforcement. This axial stress not only depends on the magnitude of the temperature change but also relates to the material properties and geometric dimensions of the reinforcement. The axial stress of reinforcement can be calculated using thermodynamic formulas, including the strain caused by temperature changes and the material's modulus of elasticity. Assuming the cross-sectional area of the bridge sample is X, the half-length is M, and there are L symmetrically distributed reinforcements with a radius of e inside, the axial stress of the reinforcement at point ζ, located at a distance A from the bridge span, can be calculated by the following formula:

$$\delta_t = \frac{(v+2)\Delta\beta \cdot \Delta S \cdot R_{Sz} R_{St}}{(v+1)(R_z + R_{tz} \cdot R_{St})} \left(1-\varsigma^{v+1}\right) \tag{8}$$

By using the ratio of the total cross-sectional area of the reinforcement to the cross-sectional area of the concrete $E_{tc}=V(\tau e^2)/X\text{-}V(\tau e^2)$, assuming that the constant related to the material properties of the reinforced concrete is represented by v, the difference in the coefficient of linear expansion between the reinforcement and concrete is represented by $\Delta\beta$; and the modulus of elasticity of the reinforcement and concrete at temperature S is represented by R_{Sz} and R_{St} respectively. The axial stress of the bridge concrete can be further calculated based on the following formula:

$$\delta_z = -\frac{E_{tz}(v+2)\Delta\beta \cdot \Delta S \cdot R_{Sz} R_{St}}{(v+1)(R_z + E_{tz} \cdot R_{St})} \left(1-\varsigma^{v+1}\right) \tag{9}$$

Assuming the axial thermal stress at the measuring point at temperature S is represented by δ^S, the temperature strain of the bridge surface concrete is represented by γ_y, the free expansion strain of the concrete is represented by t_{sg}, and the modulus of elasticity of the concrete at temperature S is represented by R_S. The axial thermal stress at the concrete measuring point can be calculated by the following formula:

$$\delta^S = (\gamma_y - \gamma_{sg}) \times R_S \tag{10}$$

4. EXPERIMENTAL RESULTS AND ANALYSIS

Figure 4 shows the thermal stress experimental values and calculated values of bridge surface concrete under different temperature conditions. The thermal stress of Specimen 1 reaches a peak of 9.4 at 120℃, then gradually decreases as the temperature continues to rise, even showing negative values, with a minimum of -1.8. At 200℃ and 240℃, the thermal stress exhibits significant fluctuations. The thermal stress of Specimen 2 gradually increases with the rise in temperature, reaching a maximum value of 3.5 at 240℃, remaining relatively stable without a noticeable downward trend. The thermal stress of Specimen 3 reaches a peak of 3.0 at 120℃, but then quickly decreases, with a minimum drop to -5.4, showing a significant negative value. The mean value shows that the overall trend of thermal stress increases before 120℃, and then generally decreases as the temperature rises. Compared with the calculated values, the experimental values are closer to the calculated values in the low-temperature range, but significantly deviate from the calculated values in the high-temperature range, especially for Specimens 1 and 3, showing a large negative deviation. By analyzing the experimental data, it can be seen that the thermal stress of bridge surface concrete exhibits nonlinear changes under different temperature conditions. The significant negative stress observed in Specimens 1 and 3 at high temperatures indicates that these specimens experienced significant thermal deformation and thermal stress release under high-temperature conditions, while Specimen 2 shows relatively stable positive stress, indicating that its material has better resistance to thermal stress under high-temperature conditions. The calculated values provide an idealized trend of thermal stress development, but in actual experiments, especially under high-temperature conditions, there are significant differences between the experimental results and the calculated values due to the complexity of material properties and structural conditions. This discrepancy arises from changes in the thermal properties of the actual materials, internal structural defects, or the non-uniformity of the temperature field, suggesting that when conducting thermal stress analysis of bridges, the actual behavior of the materials and their complex responses under high temperatures must be fully considered to improve the accuracy and reliability of numerical simulations.

The data in Figure 5 shows the comparison between the compressive reinforcement strain experimental values and calculated values of bridge specimens under different temperature conditions. At 50℃, the strain value of Specimen 1 varies significantly between the 1st and 4th loading levels, gradually decreasing from -64 to -224; the strain values of

Specimens 2 and 3 also decrease with increasing load, but compared to Specimen 1, the strain decrease of Specimen 2 is relatively moderate, reaching a minimum of -190, while Specimen 3 stops decreasing at -90. The calculated values show a linear decrease in strain with loading, with a minimum value of -136, revealing a difference from the actual experimental results. Under the 150℃ condition, the strain of Specimen 1 shows a more pronounced downward trend, reaching -230 at the 4th loading level, while the strains of Specimens 2 and 3 decrease to -220 and -140, respectively. Compared with the experimental results at 50℃, the strain values of the specimens at 150℃ are generally larger, indicating that thermal stress and deformation of the materials are more significant under high-temperature conditions. By analyzing the experimental results and calculated values, it can be seen that under the conditions of 50℃ and 150℃, the compressive reinforcement strain of the specimens generally increases significantly with the increase in temperature and loading, especially showing significant negative strain under high temperatures. This indicates that under high-temperature conditions, the compressive stress borne by the reinforced concrete structure is significantly enhanced, leading to a gradual increase in the strain of the reinforcement. The strain value of Specimen 1 is significantly greater than that of the other specimens, indicating that its material has a higher stress concentration or internal defects under high-temperature conditions, resulting in a greater strain increase. The strain values of Specimens 2 and 3 are relatively close, indicating that these two specimens have a relatively consistent thermal stress response under the influence of temperature and loading.

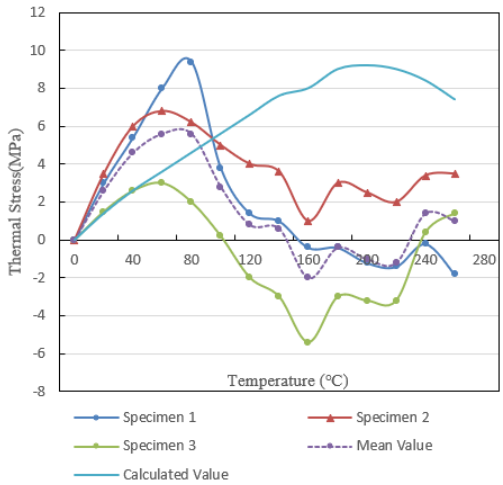

Figure 4. Thermal stress experimental values and calculated values of bridge surface concrete

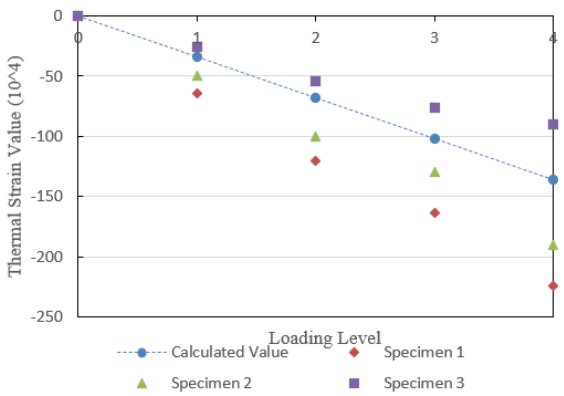

(a) 50℃

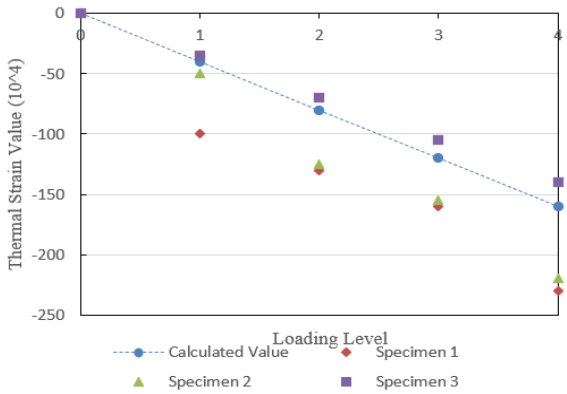

(b) 150℃

Figure 5. Compressive reinforcement strain experimental values and calculated values of bridge specimens

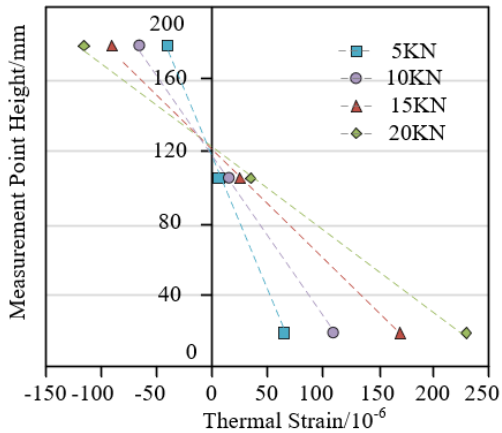

(a) 50℃

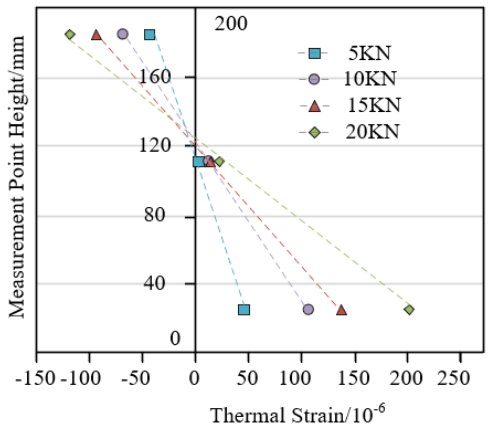

(b) 150℃

Figure 6. Distribution of thermal strain across the midspan section of bridge specimens with temperature changes

The experimental results shown in Figure 6 indicate that under different temperature conditions, the reinforced concrete structure of the bridge specimens exhibits significant strain changes. As the temperature increases, the neutral axis of the specimens gradually moves upward, indicating a redistribution of bending stress. Specifically, when the temperature reaches 110℃, the position of the neutral axis reaches its highest point, indicating that between 90℃ and 110℃, the thermal stress inside the specimen gradually accumulates and peaks within this range. This process leads to the formation of microcracks inside the concrete, which begins to release part of the thermal stress, thereby changing the stress

distribution. As the temperature further rises to 130℃, the cracks inside the concrete further expand, causing the reinforcement to start bearing more bending loads, which in turn causes the neutral axis position to gradually return to a state close to its original position. By analyzing the experimental results, it can be concluded that under high-temperature conditions, thermal stress in bridge specimens induces significant structural strain, particularly the upward movement and subsequent partial return of the neutral axis. The occurrence of this phenomenon is mainly due to stress redistribution and the formation of cracks inside the concrete caused by thermal stress accumulation. At 110℃, the neutral axis of the specimen reaches its maximum upward movement, indicating a critical point for thermal stress and structural strain, followed by a return of the neutral axis at 130℃ due to further crack development. The entire process demonstrates the complexity of material properties and structural stress responses of bridge specimens in high-temperature environments and also suggests that in practical engineering applications, special attention must be paid to the impact of high temperatures on bridge structures, particularly the issues of stress redistribution and structural deformation within critical temperature ranges.

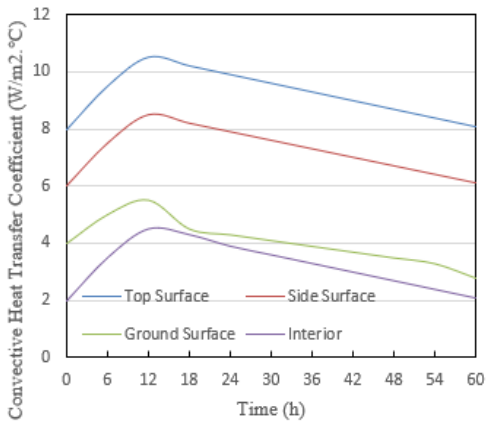

(a) 50℃

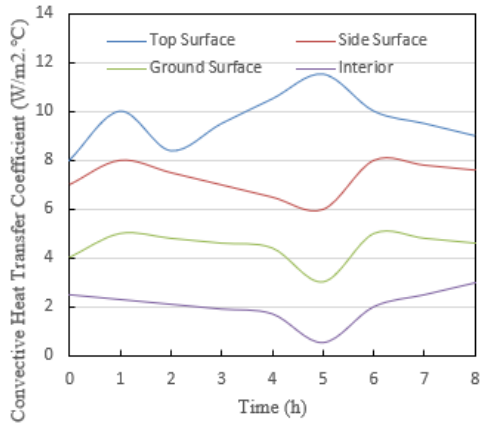

(b) 150℃

Figure 7. Calculation results of the convective heat transfer coefficient of bridge specimens

The experimental data in Figure 7 shows the changes in the convective heat transfer coefficient of the top surface, side surface, ground, and interior of bridge specimens at different time points under environmental temperatures of 50℃ and 150℃. Under the condition of 50℃, with the increase of time, the convective heat transfer coefficient at various positions shows different trends: the top surface gradually increases from the initial 8 to 10.5, reaches a peak at 12 hours, and then gradually decreases to 8.1; the side surface gradually rises from 6 to 8.5 and then also starts to decline; the convective heat transfer coefficients of the ground and interior are relatively low, rising from 4 and 2 to 5.5 and 4.5, respectively, before gradually decreasing. Under the environment of 150℃, the top surface experiences a process of first increasing and then decreasing within 8 hours, reaching a maximum of 11.5 and then gradually decreasing to 9; the side surface and ground show more complex trends, with multiple fluctuations; the convective heat transfer coefficient of the interior is relatively low and recovers after reaching a minimum value of 0.5. The experimental results show that the convective heat transfer coefficient at different positions exhibits different dynamic characteristics with changes in time and environmental temperature. Under the environment of 50℃, the convective heat transfer coefficient at various positions generally shows a trend of first increasing and then decreasing, reflecting the changes in temperature difference between the specimen surface and the surrounding air, leading to a dynamic balance of heat conduction and convective heat transfer. Under the environment of 150℃, the changes in the convective heat transfer coefficient are more intense, especially for the top and side surfaces, showing multiple fluctuations. This phenomenon is related to changes in the thermal properties of materials and the accumulation of thermal stress under high-temperature environments, leading to uneven heat flux density in local areas, which in turn affects the stability of the heat transfer process.

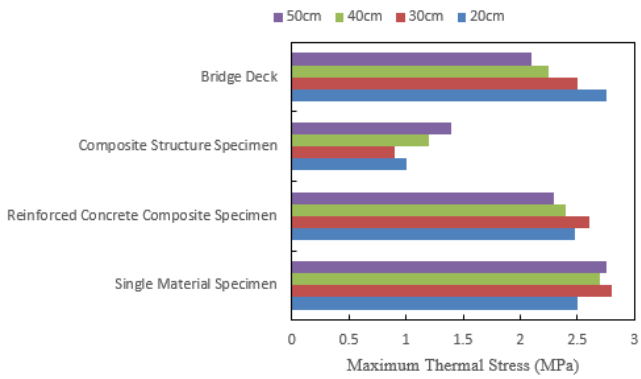

Figure 8. Maximum thermal stress of bridge specimen concrete

The data in Figure 8 shows the maximum thermal stress of different samples (single material sample, reinforced concrete composite sample, composite structure sample, and bridge deck) under different thicknesses (20 cm, 30 cm, 40 cm, 50 cm). For the single material sample, the maximum thermal stress slightly increases with the increase in thickness, from 2.5 at 20 cm to 2.8 at 30 cm, then slightly decreases to 2.7 and 2.75 at 40 cm and 50 cm, respectively. The maximum thermal stress of the reinforced concrete composite sample gradually decreases with the increase in thickness, from 2.48 to 2.3. The maximum thermal stress of the composite structure sample shows a different trend, first decreasing and then increasing with the increase in thickness, from 1 at 20 cm to 0.9 at 30 cm, then increasing to 1.2 and 1.4 at 40 cm and 50 cm, respectively. The maximum thermal stress of the bridge deck continuously decreases with the increase in thickness, from 2.75 to 2.1. Through the analysis of the experimental results, it can be

concluded that the maximum thermal stress of different samples shows different trends with the change in thickness. For the single material sample, the maximum thermal stress shows a trend of first increasing and then decreasing with the increase in thickness, indicating that in thicker materials, the accumulation of thermal stress is influenced by the internal thermal conductivity of the material. The maximum thermal stress of the reinforced concrete composite sample gradually decreases with the increase in thickness, as the reinforcement in the composite material provides better thermal diffusion paths, reducing the overall thermal stress. The maximum thermal stress of the composite structure sample shows a trend of first decreasing and then increasing, indicating the complex effect of thermal expansion mismatch between different materials within the composite material at different thicknesses. The maximum thermal stress of the bridge deck decreases with the increase in thickness, indicating that in thicker bridge decks, the release of thermal stress is more uniform. These results indicate that the thermal properties of materials and their combination methods have an important impact on the distribution of thermal stress in bridge structures and need to be given special consideration in design and simulation to ensure the durability and safety of bridge structures.

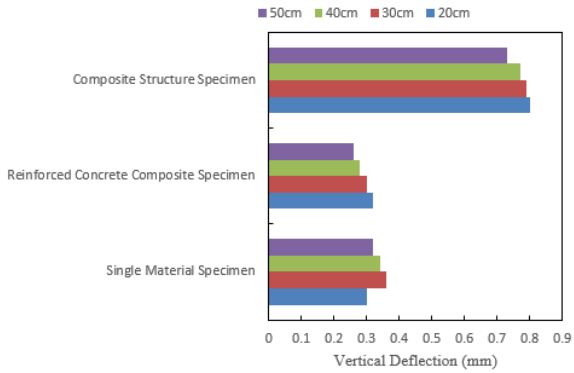

Figure 9. Vertical deflection of bridge specimens

The data in Figure 9 shows the vertical deflection of single material samples, reinforced concrete composite samples, and composite structure samples under different thicknesses (20 cm, 30 cm, 40 cm, 50 cm). For the single material sample, the vertical deflection is 0.3 at 20 cm, increases to 0.36 as the thickness increases to 30 cm, and then gradually decreases with further thickness increases, being 0.34 at 40 cm and 0.32 at 50 cm. The vertical deflection of the reinforced concrete composite sample shows a similar trend, gradually decreasing from 0.32 at 20 cm to 0.26 at 50 cm. The vertical deflection of the composite structure sample is the highest at 20 cm, being 0.8, and gradually decreases to 0.73 at 50 cm with the increase in thickness. Through the analysis of the experimental results, it can be concluded that the vertical deflection of different samples generally decreases with the increase in thickness, indicating that the increase in material thickness can effectively reduce the vertical deflection of the structure and enhance the structural stiffness. The vertical deflection of the single material sample and the reinforced concrete composite sample shows a trend of initially increasing and then gradually decreasing, as the material deformation is more significant at smaller thicknesses, while with the increase in thickness, the overall stiffness of the material increases, reducing the deformation. The vertical deflection of the composite structure sample gradually decreases with the increase in thickness, and the deflection values are relatively high, indicating that the deformation of the composite material is more significant in thinner cases, but as the thickness increases, the structural stiffness also increases.

5. CONCLUSION

This paper deeply studied the temperature changes and thermal stress distribution of bridge structures under complex climatic conditions through a thermodynamic-based numerical simulation method of bridge temperature fields. The research content includes the experimental and calculated analysis of thermal stress in bridge surface concrete, the experimental and theoretical comparison of compressive reinforcement strain, the distribution pattern of thermal strain at the midspan section of bridge specimens with temperature changes, the calculation results of the convective heat transfer coefficient of specimens, and the vertical deflection and maximum thermal stress of concrete in different structural samples under different thicknesses. The experimental and simulation results show that the thermal stress and vertical deflection distribution of bridge structures under high-temperature conditions are closely related to the thermal properties of materials, thickness, and structural combinations. Increasing the material thickness can effectively reduce vertical deflection and improve structural stiffness. At the same time, the introduction of multi-scale simulation methods improves the accuracy of temperature field simulations, providing strong theoretical support for further analysis of the thermal stress distribution of bridge structures under complex climatic conditions.

This study provides an important theoretical basis for temperature field simulation and thermal stress analysis in bridge engineering, especially under complex climatic conditions. The methods and results of this paper can help engineers more accurately predict the temperature stress and deformation of bridge structures, thereby improving the safety and durability of bridge design. However, there are also certain limitations in this study, such as the simplification in considering the changes in thermal properties of materials, and the complexity of the actual bridge environment is not fully reflected. Future research directions could consider further refining the thermal property parameters of materials and combining more complex climatic models to further improve simulation accuracy. In addition, fatigue analysis of bridge structures under long-term temperature changes could be carried out to comprehensively assess the impact of temperature on the lifespan of bridge structures.

REFERENCES

[1] Lin, J., Briseghella, B., Xue, J., Tabatabai, H., Huang, F., Chen, B. (2020). Temperature monitoring and response of deck-extension side-by-side box girder bridges. Journal of Performance of Constructed Facilities, 34(2): 04019122. https://doi.org/10.1061/(ASCE)CF.1943-5509.000139

[2] Wang, Y., Zhou, Y., Xue, Y., Yao, C., Wang, K., Luo, X. (2024). Failure analysis for overall overturning of concrete single-column pier bridges induced by temperature and overloaded vehicles. Materials, 17(11):

2650. https://doi.org/10.3390/ma17112650
[3] Zhu, Q., Wang, H., Spencer Jr, B.F. (2024). Investigation on the mapping for temperature-induced responses of a long-span steel truss arch bridge. Structure and Infrastructure Engineering, 20(2): 232-249. https://doi.org/10.1080/15732479.2022.2082494
[4] Liu, Y., Qian, Z.D., Chen, L., Hu, J. (2022). Investigation on temperature effect of bridge bearing system during steel bridge deck pavement paving. International Journal of Geomechanics, 22(5): 05022002. https://doi.org/10.1061/(ASCE)GM.1943-5622.00023
[5] Gottsäter, E., Ivanov, O.L., Molnár, M., Plos, M. (2018). Validation of temperature simulations in a portal frame bridge. Structures, 15: 341-348. https://doi.org/10.1016/j.istruc.2018.07.007
[6] Fosoul, S.A., Tait, M.J. (2023). Seismic fragility analysis of bridge-isolator-foundation-soil systems in subfreezing temperatures. Engineering Structures, 291: 116154. https://doi.org/10.1016/j.engstruct.2023.116154
[7] An, W., Shi, L., Wang, H., Zhang, T. (2022). Study on the effect of bridge deck spacing on characteristics of smoke temperature field in a bridge fire. Fire-Switzerland, 5(4): 114. https://doi.org/10.3390/fire5040114
[8] Elshoura, A., Okeil, A.M. (2024). Simplified method for estimating restraint moment induced by vertical temperature gradient in continuous prestressed concrete bridges and verification using AASHTO BDS. Structure and Infrastructure Engineering, 20(6): 944-956. https://doi.org/10.1080/15732479.2022.2132518
[9] Hussein, H.H., Khoury, I., Lucas, J.S. (2022). Environment-induced performance of end concrete diaphragm in skewed semi-integral bridges. Buildings, 12(11): 1985. https://doi.org/10.3390/buildings12111985
[10] Marchenko, A., Kromanis, R., Dorée, A.G. (2024). Characterizing bridge thermal response for bridge load rating and condition assessment: A parametric study. Infrastructures, 9(2): 20. https://doi.org/10.3390/infrastructures9020020
[11] Tesar, A., Melcer, J. (2021). Temperature conditioned resonance clusters in bridges subjected to moving loads. Civil and Environmental Engineering, 17(1): 298-302. https://doi.org/10.2478/cee-2021-0031
[12] Algohi, B., Bakht, B., Mufti, A. (2017). Long-term study on bearing restraint of a girder bridge. Journal of Civil Structural Health Monitoring, 7: 45-55.
[13] Krkoska, L., Moravcik, M. (2017). Monitoring of temperature gradient development of highway concrete bridge. In MATEC Web of Conferences, 117: 00091. https://doi.org/10.1088/1755-1315/80/1/012042
[14] Mohan, K.S.R., Sreemathy, J.R., Saravanan, U. (2017). Numerical investigation into thermal load responses of steel railway bridge. In IOP Conference Series: Earth and Environmental Science, 80(1): 012042. https://doi.org/10.1051/matecconf/201711700091
[15] Burt, D., Gonzales, J., Al-Attili, A., et al. (2019). Comparison of uniaxial and polyaxial suspended germanium bridges in terms of mechanical stress and thermal management towards a CMOS compatible light source. Optics Express, 27(26): 37846-37858. https://doi.org/10.1364/OE.27.037846
[16] Gottsäter, E., Ivanov, O.L., Molnár, M., Crocetti, R., Nilenius, F., Plos, M. (2017). Simulation of thermal load distribution in portal frame bridges. Engineering Structures, 143: 219-231. https://doi.org/10.1016/j.engstruct.2017.04.012
[17] Yang, W., You, P. (2023). Thermal stress analysis and fatigue life assessment of bridge structures under multi-physical field coupling. International Journal of Heat & Technology, 41(6): 1561-1572. https://doi.org/10.18280/ijht.410618
[18] Gaidaichuk, V., Shevchuk, L., Bilobrytska, O. (2021). Influence of incompatibility of thermomechanical parameters of bearing layers of a bridge structure on its thermo-stressed state. Strength of Materials and Theory of Structures, (107): 301-311. https://doi.org/10.32347/2410-2547.2021.107.301-311
[19] Heymsfield, E., Murray, C.D., Salah, A.A., Benitez-Ortiz, F. (2024). Evaluating the continuous deck placement sequence approach at steel bridges using a time-dependent numerical analysis. Journal of Performance of Constructed Facilities, 38(5): 04024028. https://doi.org/10.1061/JPCFEV.CFENG-4473
[20] Lou, P., Wang, Q., Au, F.T.K., Cheng, Y.W., Yan, B., Xu, Q.Y. (2020). Finite element analysis of the thermal interaction of continuously welded rails with simply supported bridges considering nonlinear stiffness. Proceedings of the Institution of Mechanical Engineers, Part F: Journal of Rail and Rapid Transit, 234(10): 1358-1367. https://doi.org/10.1177/0954409719896471
[21] Nariman, N.A. (2018). Thermal fluid-structure interaction and coupled thermal-stress analysis in a cable stayed bridge exposed to fire. Frontiers of Structural and Civil Engineering, 12: 609-628. https://doi.org/10.1007/s11709-018-0452-z